RadioGraphics

MR Imaging and MR Arthrography of the Postoperative Shoulder: Spectrum of Normal and Abnormal Findings[1]

Aurea V. R. Mohana-Borges, MD • Christine B. Chung, MD
Donald Resnick, MD

ONLINE-ONLY CME

See www.rsna.org/education/rg_cme.html.

LEARNING OBJECTIVES

After reading this article and taking the test, the reader will be able to:

- Recognize the normal or abnormal appearance of the shoulder at follow-up MR imaging after common surgical repairs for impingement syndrome and instability.
- Identify common complications depicted on MR images of the postoperative shoulder.
- Describe the advantages and limitations of various MR imaging techniques and sequences for evaluation of the postoperative shoulder.

The postoperative shoulder may be evaluated with various imaging modalities, including radiography, ultrasonography, computed tomography, and magnetic resonance (MR) imaging, each of which has advantages and disadvantages. For optimal soft-tissue visualization, MR imaging and MR arthrography are widely used. Several factors, however, may decrease the accuracy of MR imaging in the evaluation of the postoperative shoulder. These factors include surgical distortions of native anatomy, changes in the signal intensity of tissues, and image degradation caused by metallic artifacts. To maximize the accuracy of MR imaging, the radiologist must select the most appropriate pulse sequences and techniques for the given anatomic structure and the suspected postoperative condition. To avoid magnetic susceptibility artifacts at MR imaging, inversion recovery may be used instead of fat saturation, and fast spin-echo sequences may be used instead of conventional spin-echo sequences or gradient-echo sequences. MR arthrography is most useful for optimal delineation of the rotator cuff, capsulolabral structures, and tendon defects. To achieve accurate image interpretation, the radiologist must be familiar with the arthroscopic and the open surgical techniques currently used to repair internal derangements of the glenohumeral joint, as well as with the typical imaging findings in each postoperative situation.

Index terms: Magnetic resonance (MR), arthrography, 41.12143 • Shoulder, injuries, 41.40 • Shoulder, MR, 41.12141 • Shoulder, surgery, 41.45

RadioGraphics 2004; 24:69–85 • **Published online** 10.1148/rg.241035081

[1]From the Department of Radiology, Veterans Administration Medical Center, 3350 La Jolla Village Dr, San Diego, CA 92161. Presented as an education exhibit at the 2002 RSNA scientific assembly. Received March 25, 2003; revision requested April 28 and received June 16; accepted June 18. All authors have no financial relationships to disclose. **Address correspondence to** C.B.C. (e-mail: *cbchung@ucsd.edu*).

Introduction

The postoperative shoulder may be evaluated with various imaging modalities, including radiography, ultrasonography (US), computed tomography (CT), and magnetic resonance (MR) imaging, each of which has advantages and disadvantages. Radiography is adequate for the evaluation of prostheses, bone alignment, and surgical hardware, but it has very low sensitivity and specificity for the evaluation of soft tissues. US is adequate in evaluation of the soft tissues in the rotator cuff but is operator dependent and has limitations in the evaluation of labral and bone abnormalities. CT provides high-resolution depiction of osseous structures, as well as high-quality multiplanar imaging capabilities. MR imaging is the modality of choice for obtaining optimal soft-tissue visualization; however, several factors, described later in this article, may decrease its accuracy in the evaluation of the postoperative shoulder.

The most frequently performed surgical procedures followed up with MR imaging of the shoulder are subacromial decompression for impingement, rotator cuff repair, and repair of glenohumeral instability (1). Surgical procedures may be accomplished with either open or arthroscopic techniques. For rotator cuff repairs and acromioplasty, surgical intervention requires detachment of the deltoid muscle from the acromion, whereas arthroscopy requires only the creation of small incisions for the insertion of arthroscopic instruments. Advantages of open surgical procedures include ease of performance without special equipment, direct visualization of cuff repair and acromioplasty, and good long-term results. Major disadvantages include the necessity of detaching the deltoid muscle, which increases perioperative morbidity, and the inability to access intraarticular abnormalities other than very large rotator cuff tears (2,3). The increasing use of arthroscopic procedures has been spurred by the advantages of arthroscopy over open surgery, which include a smaller surgical scar, less-severe postoperative pain, fewer complications, and faster postoperative rehabilitation.

For orthopedic surgeons who are less familiar with arthroscopy than with open surgery, "mini-open" procedures may be an attractive alternative to purely arthroscopic procedures (4). In rotator cuff repairs, the hybrid procedure is performed by making a small incision between the anterior and lateral heads of the deltoid muscle to achieve exposure of the rotator cuff tendons without excessive destruction of the acromion or detachment of the deltoid muscle. Mini-open procedures combine advantages of open repair (direct visualization, long-term success rates) with those of arthroscopy (visualization of intraarticular abnormalities, decreased morbidity). Mini-open procedures may be an effective transitional stage in the long-term refinement and dissemination of purely arthroscopic surgical techniques (4).

The increasing use both of arthroscopic and of open surgical techniques to repair internal derangements of the glenohumeral joint necessitates a thorough and up-to-date understanding of common MR imaging findings in the postoperative shoulder. This article surveys conventional and new surgical procedures for the repair of shoulder impingement and instability; describes normal and abnormal findings at postoperative follow-up imaging; and compares the advantages and limitations of different MR imaging techniques and sequences in evaluation of the postoperative shoulder.

Surgical Repair of Shoulder Impingement and Instability

In general, shoulder surgery is considered only when conservative therapy fails. Surgery may be indicated when dislocation occurs repeatedly during light activity that involves overhead extension of the shoulder. Rotator cuff repair is considered when there is severe pain and loss of function in the shoulder. A shoulder prosthesis may be necessary in patients with severe fractures of the humeral head that compromise the blood supply to the articular surface or with osteonecrosis of the humeral head, dislocation and significant fracture of the articular surface, or severe and painful arthritis (1–3). Surgery is contraindicated in the presence of infection or other serious illness.

Impingement

Arthroscopic subacromial decompression is currently the method of choice for treatment of chronic extrinsic impingement of tendons in the rotator cuff. The main advantage of arthroscopic

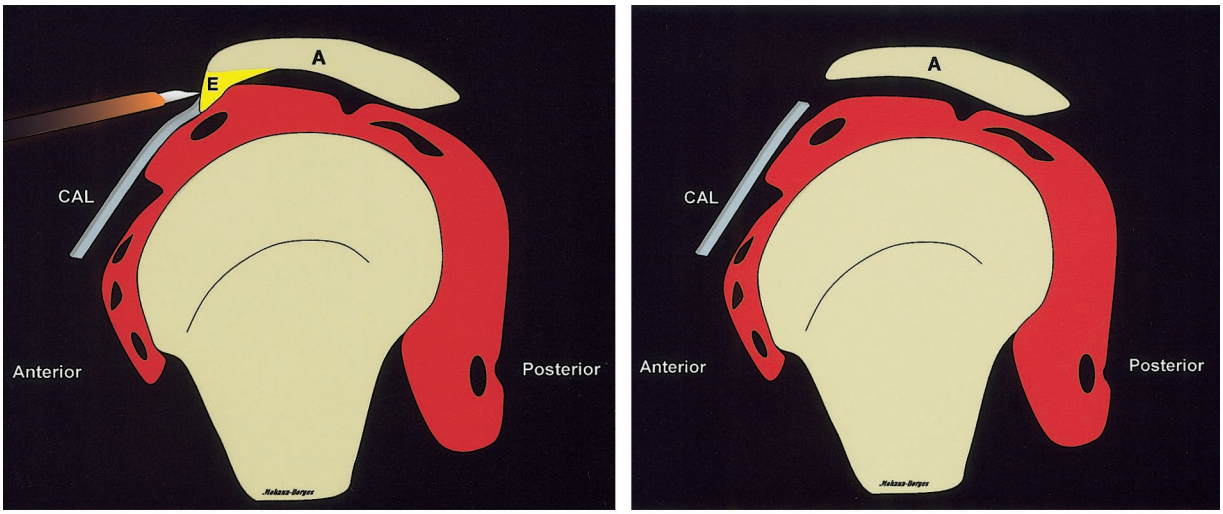

a. b.

Figure 1. Schematics in the sagittal plane show acromial morphology before **(a)** and after **(b)** subacromial decompression. **(a)** Subacromial enthesophyte (*E*) projects from the anteroinferior surface of the acromion (*A*) and impinges on the adjacent rotator cuff tendon. Note the relationship of the subacromial enthesophyte to the coracoacromial ligament (*CAL*). **(b)** After surgery, the curved undersurface of the acromion (*A*) is flatter. Resection of the coracoacromial ligament (*CAL*) is represented by the absence of acromial attachment. (Compare with Fig 8.)

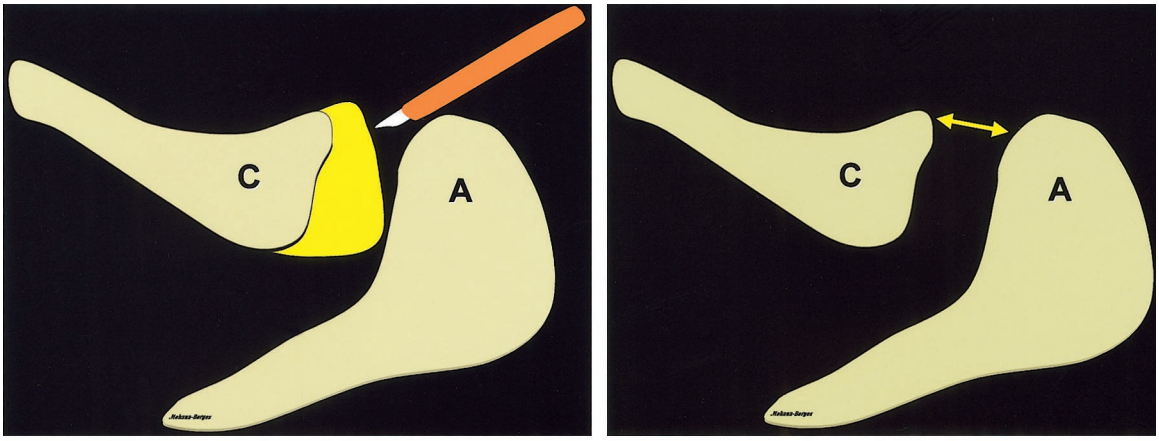

a. b.

Figure 2. Schematics in the axial plane show clavicular morphology before **(a)** and after **(b)** the Mumford procedure. **(a)** Note the proximity of the distal part of the clavicle (*C*) to the acromion (*A*) prior to the procedure. **(b)** With resection of the distal part of the clavicle, acromioclavicular distance increases 1–2 cm. (Compare with Fig 9.)

decompression over open acromioplasty is the greater preservation of both the deltoid muscle and the overlying deltotrapezial fascia (1). The primary goal of the procedure is to make more space available for the tendons of the rotator cuff. Enlargement, or decompression, of the space between the acromion and the humeral head can relieve the symptoms of impingement. Briefly, arthroscopic subacromial decompression consists of diagnostic arthroscopy, resection of the coracoacromial ligament, anterior and posterior acromion resection, resection of acromioclavicular joint osteophytes, and, if necessary, distal clavicular resection (the Mumford procedure) (Figs 1, 2).

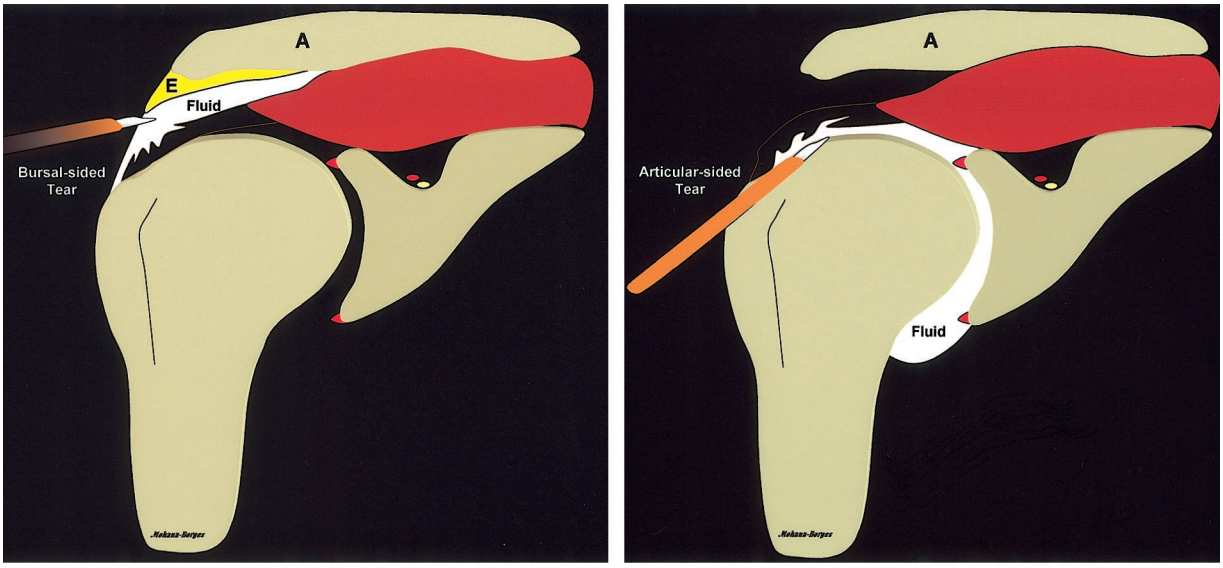

a. b.

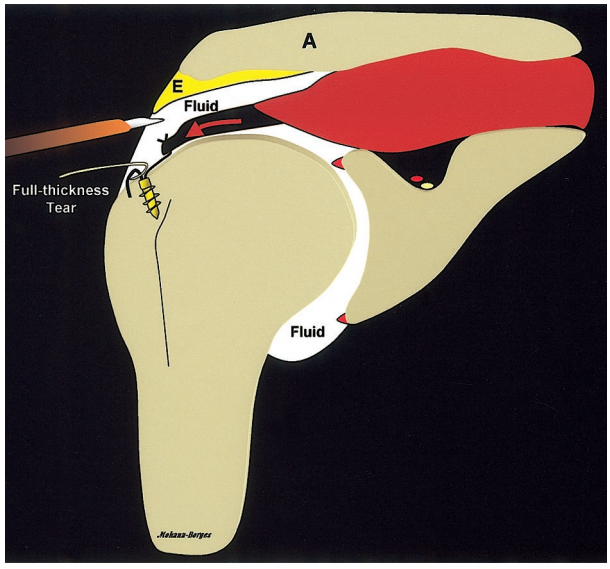

c.

Figure 3. Schematics in the coronal plane show the typical results of surgical repair of bursal-sided **(a)**, articular-sided **(b)**, and full-thickness **(c)** tears of the rotator cuff. *A* = acromion, *E* = enthesophyte.

Arthroscopic findings associated with impingement include fraying of the articular or bursal surface of the rotator cuff, subacromial-subdeltoid bursitis, acromioclavicular arthritis, and evidence of fraying of the coracoacromial ligament where it attaches to the anteroinferior surface of the acromion. These findings are depicted on MR images as areas of irregularity and increased signal intensity in the tendons of the rotator cuff, fluid in the subacromial-subdeltoid bursa, acromioclavicular bone proliferation and osteophytes, and thickening and irregularity of the coracoacromial ligament (5).

Rotator Cuff Tears

Optimal management of rotator cuff disease varies according to the presence and severity of impingement, degree of tendon tear, and functional demands. Partial bursal-sided tears, especially those associated with morphologic changes in the coracoacromial arch (eg, type 2 or 3 acromion, subacromial enthesophyte), respond favorably to arthroscopic subacromial decompression and débridement. Partial articular-sided tears that do not involve more than two-thirds of the tendon

Open Surgical Procedures Commonly Used for Glenohumeral Joint Instability

Procedure	Technique	Effects	Complications
Bankart*	Repair of inferior glenohumeral ligament complex with drill holes and sutures	Anatomic repair with limitation of external rotation	None
Putti-Platt	Shortening of the anterior capsule and subscapularis muscle	Nonanatomic soft-tissue repair with limitation of external rotation	Degenerative joint disease, overlimitation of external rotation
Magnusson-Stack	Transfer of the subscapularis tendon from the lesser to the greater tuberosity	Nonanatomic soft-tissue repair with limitation of external rotation	Overlimitation of external rotation
Bristow-Helfet	Transfer of the coracoid process with its attached tendons to the neck of the scapula	Nonanatomic bone-block repair with limitation of external rotation and prevention of anterior displacement of the humeral head	Nonunion, migration, recurrence, missed labral tears
Bone-block osteotomy	Anterior bone block	Nonanatomic bone-block repair with prevention of anterior displacement of the humeral head	Nonunion, migration, recurrence, articular injury
Neer capsular shift†	Inferior capsule shifted in the superior direction	Capsular tightening	Overtightening

*The Bankart procedure is the standard treatment for Bankart lesion.
†Neer capsular shift is the standard treatment for multidirectional instability.

thickness also respond well to débridement of the necrotic torn tissue, with or without anterior acromioplasty. Full-thickness tears generally require open surgery, although arthroscopy-assisted (mini-open) rotator cuff repairs and purely arthroscopic repairs are possible in some tears (Fig 3) (6).

Briefly described, mini-open rotator cuff repair involves splitting the deltoid muscle without detaching it from the acromial edge, débridement of any unhealthy rotator cuff tissue, side-to-side suturing of the torn ends, and reattachment of the tendon to the greater tuberosity with sutures anchored to various fixation devices. Acromioplasty and the Mumford procedure are usually performed to increase the space under the acromion (1,2).

Instability

Many different surgical procedures, open and arthroscopic, have been used to repair the capsulolabral complex and to strengthen the glenohumeral ligaments in patients with posttraumatic glenohumeral joint instability. Open surgical techniques can be classified as either anatomic or nonanatomic reconstructions (Table). Anatomic reconstructions, which are most commonly performed, are repairs that do not alter the native

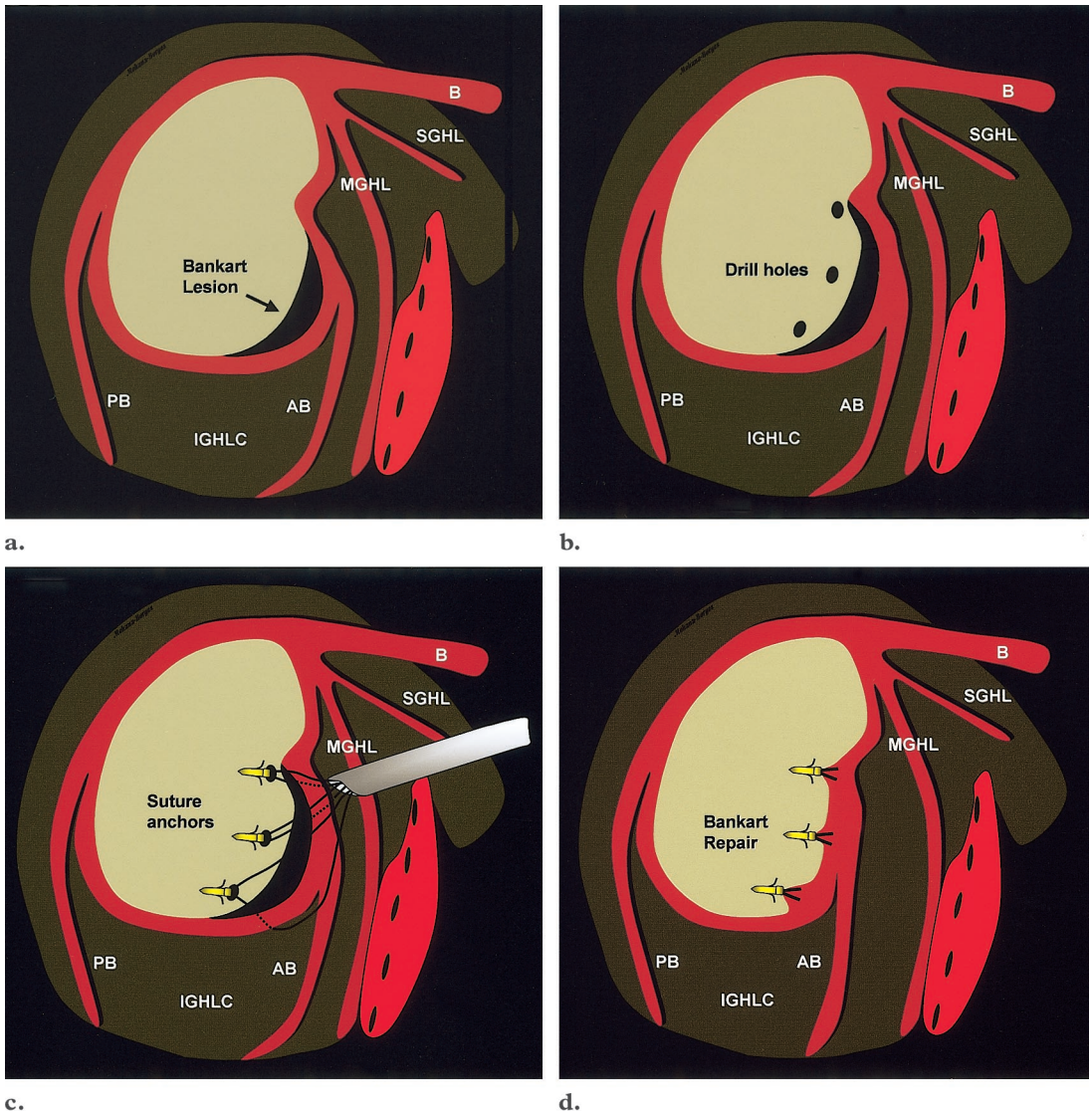

Figure 4. Schematics in the sagittal plane show Bankart lesion before **(a)**, during **(b, c)**, and after **(d)** surgical treatment. **(a)** Bankart lesion is represented by separation of the anteroinferior labrum from the glenoid bone (arrow). **(b)** Holes are drilled in the glenoid bone at 3-, 4-, and 5-o'clock positions. **(c)** Suture anchors are passed through the drill holes. **(d)** The labrum is reattached to the glenoid bone. *AB* = anterior band of the inferior glenohumeral ligament complex, *B* = biceps tendon, *IGHLC* = inferior glenohumeral ligament complex, *MGHL* = middle glenohumeral ligament, *PB* = posterior band of the inferior glenohumeral ligament complex, *SGHL* = superior glenohumeral ligament.

anatomy of the shoulder. Examples are Bankart repair, in which three suture anchors are passed through holes drilled in the bone at approximate 3-, 4-, and 5-o'clock positions (Fig 4), and Du Toit and Roux staple capsulorrhaphy, which is used less often than Bankart repair because of a high rate of fixation failure (6).

Nonanatomic reconstructions, which are no longer commonly used except in revision surgery, are classified according to whether they involve soft tissues or osseous structures (5,7). Soft-tissue reconstructions such as the Putti-Platt (Fig 5) and Magnusson-Stack procedures involve indirect tightening of the capsule with manipulation of the subscapularis tendon (3) (Table). Bone-

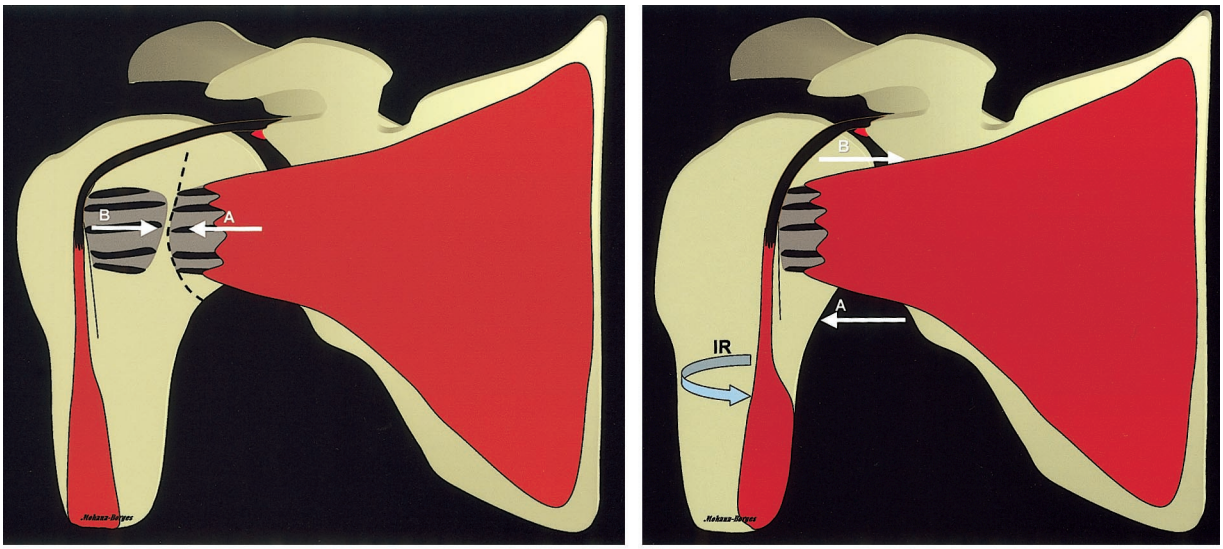

a. b.

Figure 5. Schematics of the Putti-Platt procedure. **(a)** In the first stage of the procedure, parts of the anterior capsule and tendons *A* and *B* of the subscapularis muscle are resected and shortened. **(b)** In the second stage, the lateral tendon stump (*B*) is attached to the most accessible soft-tissue structure along the anterior rim of the glenoid cavity. The medial tendon stump (*A*) is overlapped with the lateral tendon stump and reattached to the lesser tuberosity of the humerus. *IR* = internal rotation of the humerus.

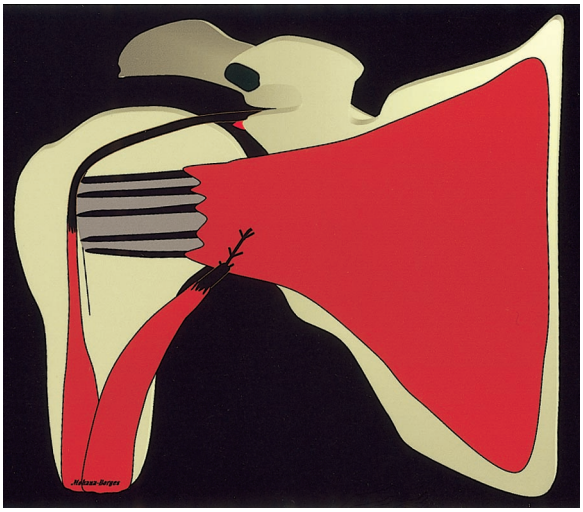

Figure 6. Schematic of the Bristow-Helfet procedure. The coracoid process and the short head of the biceps tendon are transferred to the anteroinferior glenoid rim through the split subscapularis tendon.

block osteotomies such as the Bristow-Helfet procedure mechanically prevent or block recurrent anterior dislocation of the glenohumeral joint with a graft of the coracoid process or other bone to the anteroinferior glenoid rim through a split in the subscapularis tendon (Fig 6).

Inferior capsular shift is a soft-tissue reconstruction procedure that is performed to thicken and tighten the capsule (Fig 7). First, a T-shaped incision is made in the capsule. Then the inferior part of the capsule is advanced (shifted) in a superior direction and the superior part of the capsule is advanced in the anteroinferior direction until the two overlap at the point of greatest instability. The margins of the incision are then sutured to hold the overlapping parts of the capsule in place, providing increased thickness in the anteroinferior part of the capsule and greater tension on the humeral side. This procedure has been used both as a primary treatment for multidirectional instability and as an adjuvant to Bankart repair in patients with significant capsular laxity (1) (Table).

The effectiveness of arthroscopic surgery for glenohumeral instability is not yet fully known, but arthroscopic techniques might predictably be most effective in young patients who have traumatic dislocations without systemic joint laxity and who do not participate in contact sports. Popular arthroscopic methods of fixation include transglenoid sutures (Caspari, Morgan, Maki), absorbable tacks (Warren), and suture anchors (Snyder and others) (6).

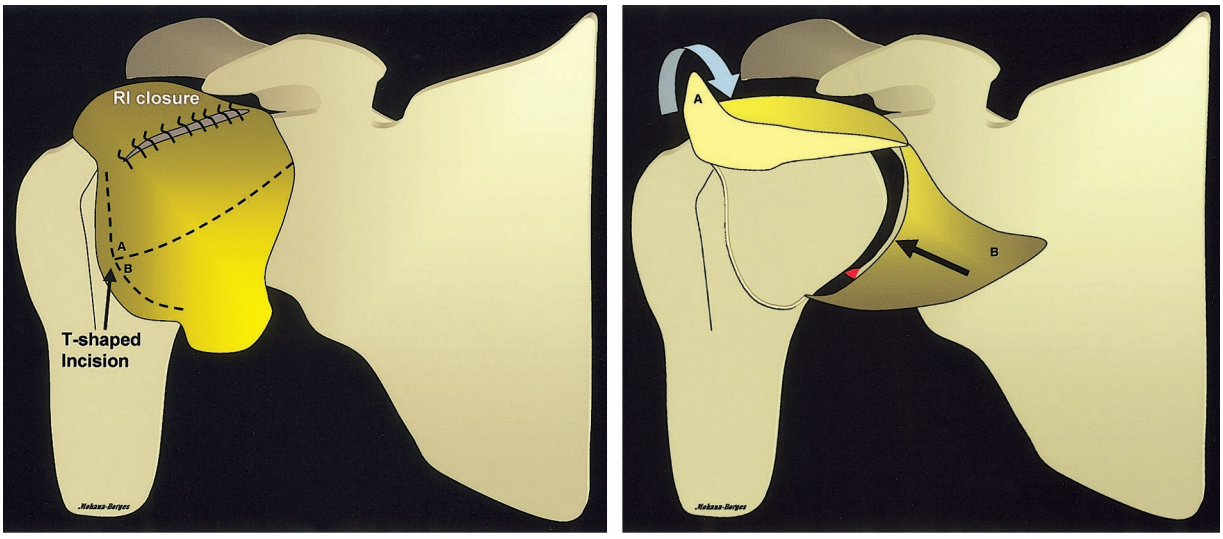

a. b. c.

Figure 7. Schematics of the capsular shift procedure. **(a)** A horizontal T-shaped incision is made in the anterior part of the capsule. Note the closure of the rotator interval (*RI*). **(b)** The inferior part of the capsule (*B*) is shifted in the superior direction, and the superior part of the capsule (*A*) is shifted in the anteroinferior direction to overlap it. **(c)** The margins of the incision are sutured to hold the overlapping parts of the capsule together.

The application of laser and thermal energy in arthroscopic shoulder surgery remains controversial. At present there is a lack of basic science research and controlled prospective clinical research in this area. The specific capabilities of the laser (tissue ablation and restoration of homeostasis) make it a useful tool in arthroscopic shoulder surgery, particularly for ablation of hypertrophic synovium (ie, synovectomy). Laser ablation also has been applied to the subacromial space and glenohumeral joint for the débridement of labral lesions, release of the coracoacromial ligament, and chondroplasty. In addition, anecdotal reports of the use of lasers to shrink the capsular tissue in patients with glenohumeral joint instability have led to the development of the phrase "laser-assisted capsular shift" to describe laser-induced change in the morphology of the shoulder capsule (8). Thermal shrinkage has become immensely popular, particularly because conventional capsular shift procedures cannot be performed with arthroscopic techniques.

Normal and Abnormal Findings at Postoperative MR Imaging

Expected findings at MR imaging after arthroscopic subacromial decompression include morphologic changes in the acromion and the coracoacromial ligament (Fig 8) and widening of the acromioclavicular distance (Fig 9). Postoperative imaging of the coracoacromial arch, like preoperative imaging, is most often performed in the sagittal plane. However, changes in the appearance of the acromion and coracoacromial ligament on images obtained in this plane may be subtle, and comparison with preoperative studies is strongly recommended. The shape of the acro-

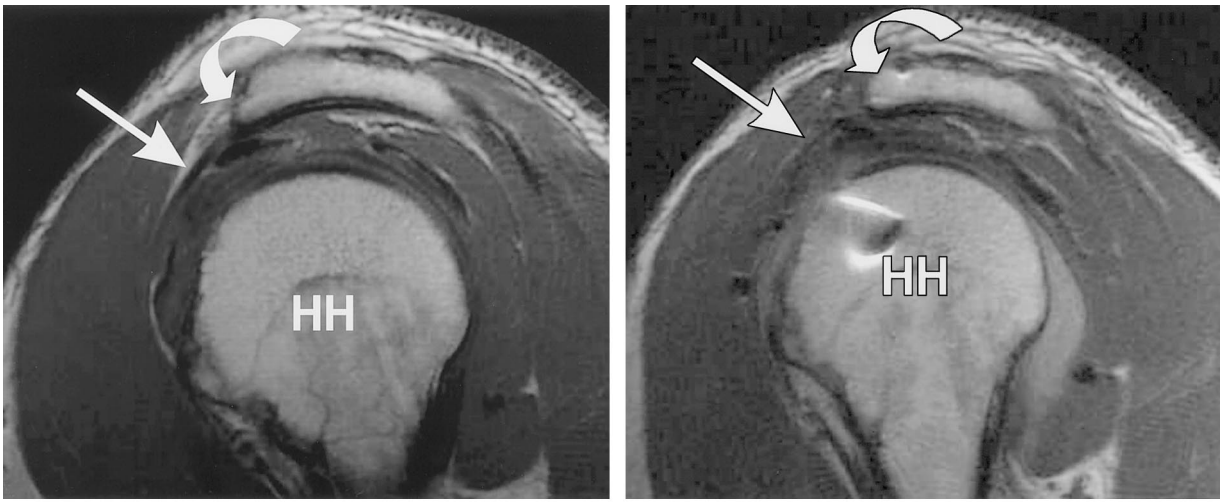

a. **b.**

Figure 8. Sagittal T1-weighted (500/12) images show the morphology of the coracoacromial ligament (straight arrow) and the acromion (curved arrow) before **(a)** and after **(b)** coracoacromial ligament resection and anterior acromioplasty. (Compare with Fig 1.) *HH* = humeral head.

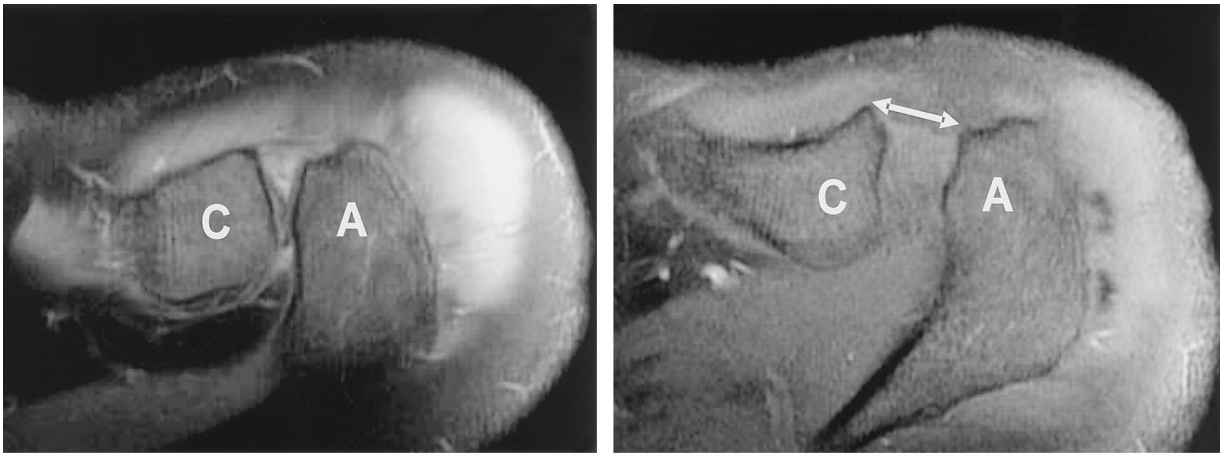

a. **b.**

Figure 9. Subacromial decompression (Mumford procedure). **(a)** Axial proton-density–weighted (2,800/10) fat-suppressed image shows the proximity of the distal part of the clavicle (*C*) to the acromion (*A*). **(b)** T1-weighted fat-suppressed image obtained after resection of the distal part of the clavicle shows an increase of 1–2 cm in the acromioclavicular distance. (Compare with Fig 2.) *A* = acromion, *C* = clavicle.

mion usually changes from a hook or curve to a flatter and slightly tapered configuration. Decreased signal intensity in the acromion on both short-echo-time (T1- or proton-density–weighted) and long-echo-time (T2-weighted) images represents fibrosis in the acromial marrow (1). After resection, the coracoacromial ligament may be replaced at the site of its former attachment to the acromion by fat tissue and may not be visible on MR images. This site also might have abnormal signal intensity and an irregular morphology caused by scar tissue and metallic artifacts. Widening of the acromioclavicular distance by 1–2 cm has been associated with resection of osteophytes or hypertrophic bone (Mumford procedure) (1). Residual tendon degeneration or tear and acromioclavicular osteoarthrosis also may be present and may become apparent during correlation of postoperative images with preoperative images (5,6,9,10).

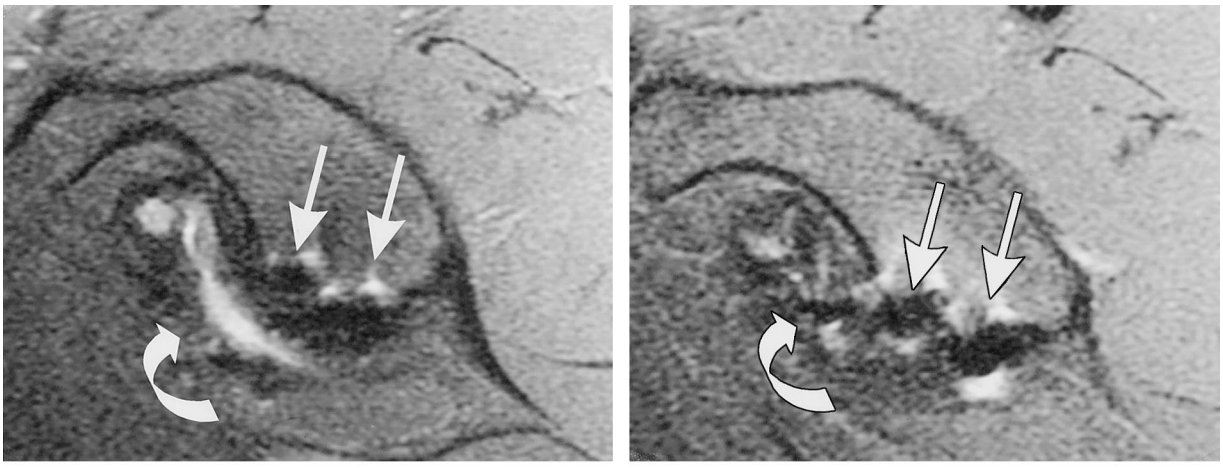

a. **b.**

Figure 11. Bankart repair 2 years previous in a 37-year-old man. Sagittal T1-weighted (600/13) fat-suppressed MR arthrograms (**b** more medial than **a**) depict capsular thickening (curved arrow) and metallic artifacts (straight arrows) from suture anchors in the anteroinferior glenoid quadrant.

Expected findings at MR imaging after rotator cuff repair include either intermediate or low signal intensity in the tendon (indicating granulation tissue and fibrosis, respectively) and regular or irregular morphology, depending on the procedure performed and the quality of the remaining tendon (Fig 10) (1,6). According to a preliminary study in 15 asymptomatic patients, only 10% of repaired tendons have a normal appearance at MR imaging (11). These preliminary results support the use of MR arthrography in the routine assessment of rotator cuff tendon repairs.

Mild superior subluxation of the humeral head may be caused by capsular tightening, scarring, cuff atrophy, or bursectomy. Fluid in the subacromial-subdeltoid space is a nonspecific postoperative finding that may be associated with a functional nonwatertight repair, a recurrent tear in the rotator cuff, or an otherwise normal postoperative rotator cuff (11). Extension of this fluid to the acromioclavicular joint (with or without recurrent rotator cuff tendon tear), indicated by the geyser sign on postoperative MR images, is a common finding secondary to injury of the acromial undersurface during surgery.

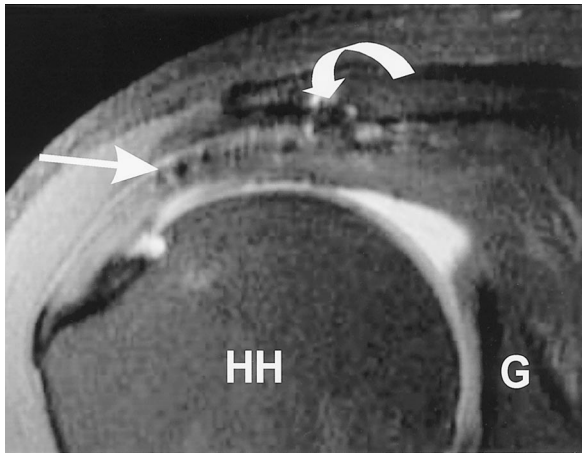

Figure 10. Rotator cuff repair and arthroscopic subacromial decompression in a middle-aged man. Coronal T1-weighted (500/12) fat-suppressed MR arthrogram shows intact supraspinatus tendon. Note the artifacts in the area of the repaired tendon (straight arrow) and the undersurface of the acromion (curved arrow). *G* = glenoid, *HH* = humeral head.

Expected findings after Bankart repair are the presence of paramagnetic artifacts or anchor tracks (with the number depending on the quantity of anchors used at surgery) in the anterior glenoid bone (Fig 11) and the reattachment of the capsulolabral complex to the glenoid margin. In

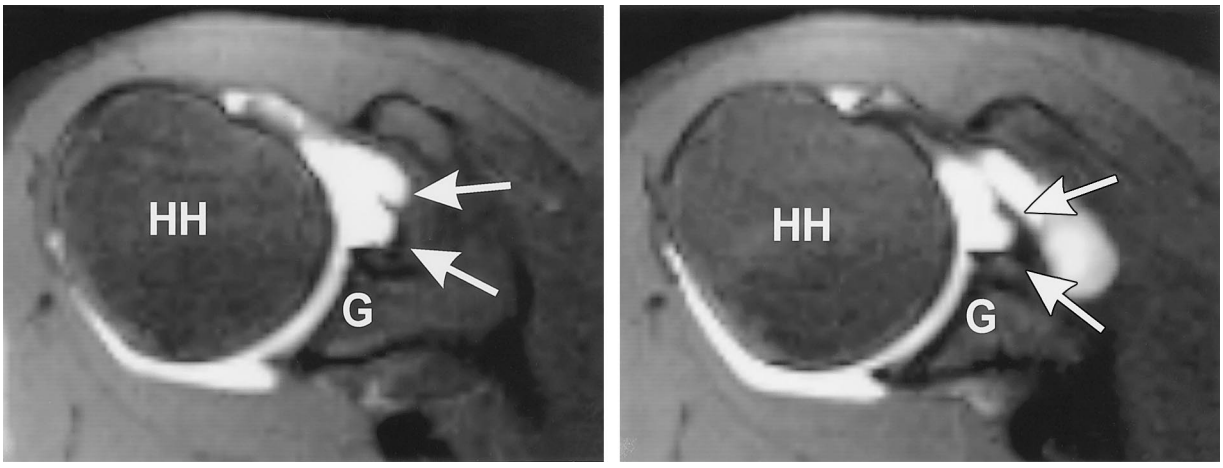

a. **b.**

Figure 13. Repair of superior labral anterior-to-posterior tear in a middle-aged woman. Axial T1-weighted (450/12) fat-suppressed sequential images (**a** at a higher level than **b**) show postoperative thickening of the superior glenohumeral ligament and rotator interval capsule (arrows). *G* = glenoid, *HH* = humeral head.

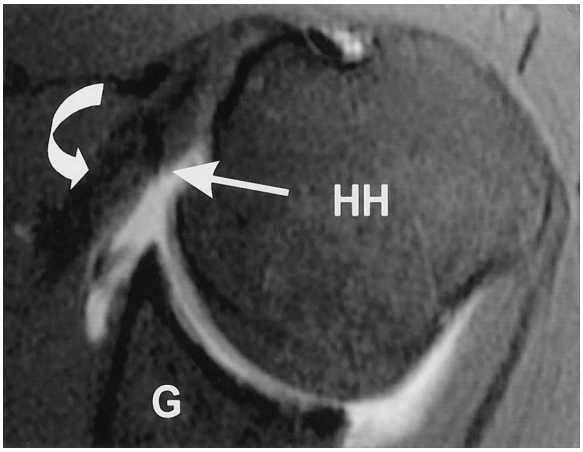

Figure 12. Capsular shift procedure in a middle-aged man. Axial T1-weighted (500/12) fat-suppressed MR arthrogram shows postoperative thickening of the anteroinferior part of the capsule (straight arrow) and overlying subscapularis tendon (curved arrow). *G* = glenoid, *HH* = humeral head.

nonanatomic reconstructions, labral and capsular lesions are not directly repaired, and abnormalities due to these lesions are still visible on postoperative MR images (6). Capsular thickening is another common finding after surgical repairs of instability and labral tears (Figs 11–13) (12,13). This finding may be directly associated with the procedure performed (eg, capsular shift, capsular plication, or laser capsular shrinkage) or caused by scar tissue in the area of the surgical incision. Marked thickening of the subscapularis tendon at the site of attachment to the lesser tuberosity has been described in patients who have undergone the Putti-Platt procedure (12). On follow-up images obtained after the Bristow-Helfet procedure, alterations in the coracoid process and anterior glenoid margin have been noted. All postoperative imaging findings should be correlated with the specific procedure performed.

Common Intraoperative and Postoperative Complications

Intraoperative complications may include fracture of the acromion, unintended detachment or dehiscence of the deltoid muscle (Fig 14), axillary nerve injury with subsequent denervation of the deltoid and teres minor muscles, and failure to preserve the coracoacromial arch in patients who have an irreparable tear in the rotator cuff (14). The axillary nerve may be injured during various surgical procedures and at various sites (Fig 15).

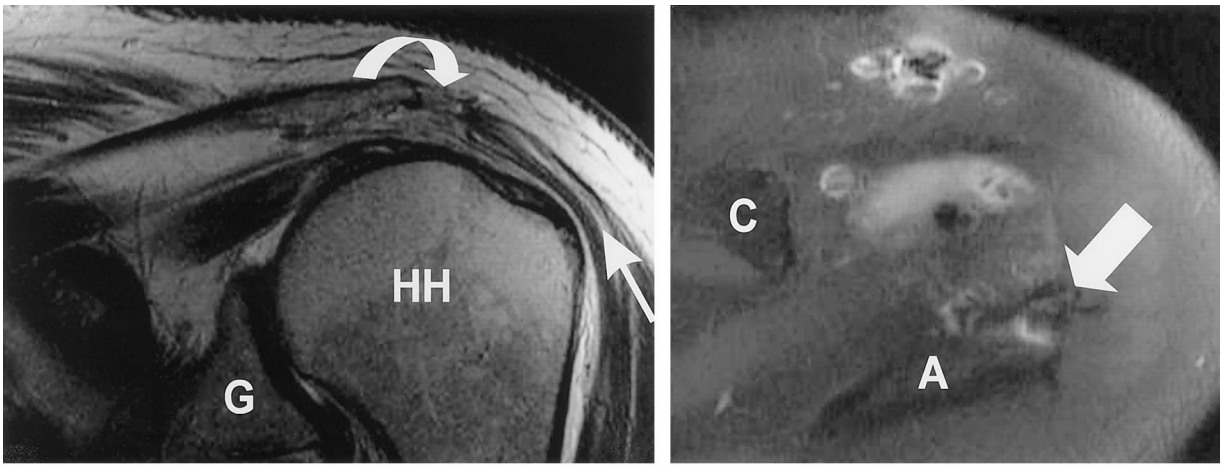

a. **b.**

Figure 14. Mumford procedure in a young man. **(a)** Coronal T2-weighted fast spin-echo image depicts fatty atrophy (straight arrow) and dehiscence (curved arrow) of the deltoid muscle. **(b)** Axial T1-weighted fat-suppressed image shows extensive acromioplasty (arrow), a probable cause of deltoid muscle abnormalities identified in this patient. *A* = acromion, *C* = clavicle, *G* = glenoid, *HH* = humeral head.

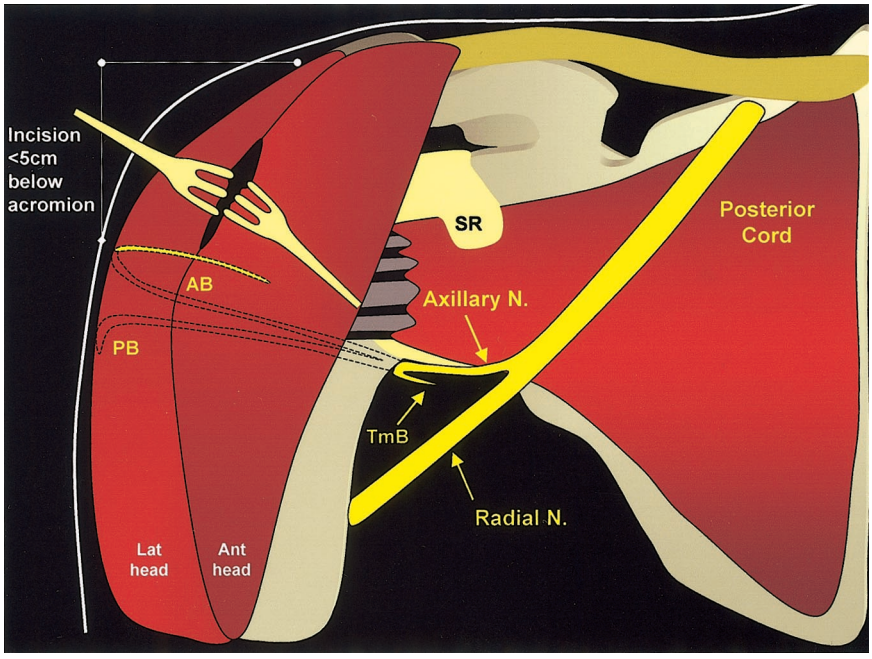

Figure 15. Schematic representation of the axillary nerve and its correlation with shoulder surgeries. The axillary nerve originates from the posterior cord of the brachial plexus and crosses the inferolateral surface of the subscapularis muscle and the inferior glenohumeral joint capsule, where it is vulnerable to injury during surgery for glenohumeral instability. From here it branches through quadrilateral space to the teres minor muscle (*TmB*). At the posterior surface of the humerus, the nerve divides into a posterior branch (*PB*) and an anterior branch (*AB*). The anterior branch curves downward to innervate the lateral and anterior heads of the deltoid muscle. At these sites the nerve is vulnerable to injury during open subacromial decompression surgery and rotator cuff repair if the deltoid muscle is split anteriorly for a distance greater than 5 cm. *Ant* = anterior, *Lat* = lateral, *N.* = nerve, *SR* = subscapular recess.

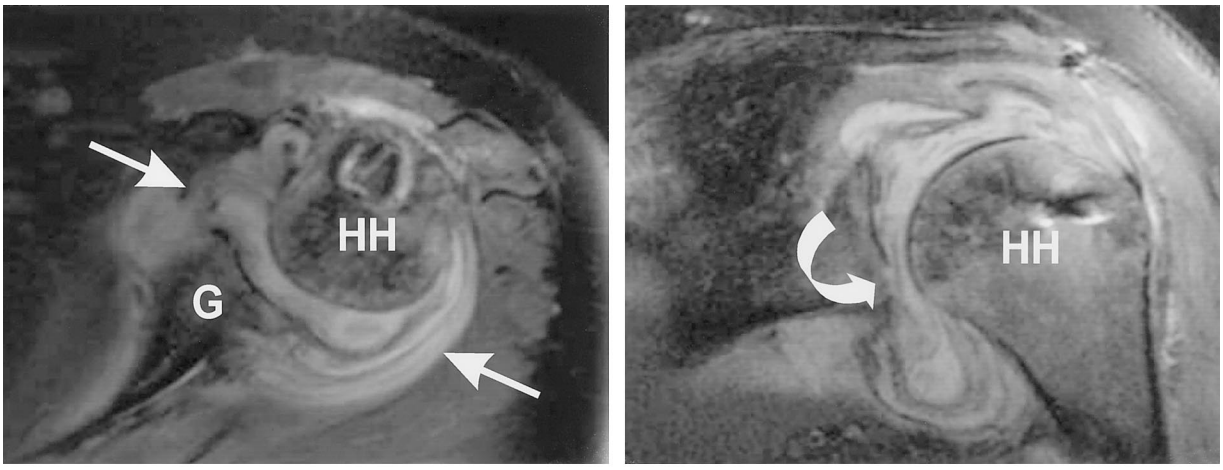

a. **b.**

Figure 16. Septic arthritis in a 47-year-old woman with progressive shoulder pain for 2 months after rotator cuff repair. Axial **(a)** and coronal **(b)** T1-weighted fat-suppressed images obtained with intravenous administration of gadolinium-based contrast material show synovial, capsular, and soft-tissue enhancement (arrows in **a**), marginal erosion (arrow in **b**), and capsular laxity. Note the high-grade partial tear of the supraspinatus tendon in **b**. *G* = glenoid, *HH* = humeral head.

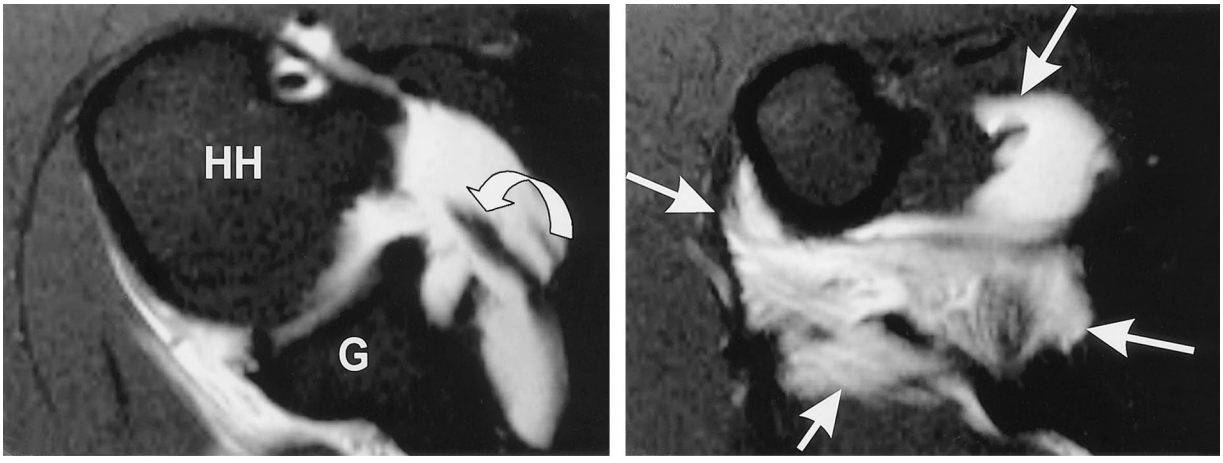

a. **b.**

Figure 17. Subscapularis tendon tear and capsular rupture in a 17-year-old male patient after arthroscopic surgery. Axial T1-weighted fat-suppressed MR arthrograms show the tear (arrow in **a**) and extravasation of contrast material (arrows in **b**) into soft tissues around the capsule, in the region of the axillary pouch. *G* = glenoid, *HH* = humeral head.

In open subacromial decompressions and rotator cuff repairs, the anterior branch of the axillary nerve might be damaged if the deltoid muscle is split anteriorly for a distance greater than 5 cm. During surgery for glenohumeral instability, the axillary nerve adjacent to the inferior border of the joint capsule and subscapularis muscle might be damaged.

Short-term postoperative complications may include hematoma, infection, and septic arthritis (Fig 16). In addition, overly intense physical therapy during patient rehabilitation in the early postoperative period may lead to avulsion of tendons or capsular structures. The persistence of signs of impingement, however, usually is related to inadequate acromioplasty (14).

Long-term postoperative complications may include recurrent tear in the tendons of the rotator cuff and capsulolabral structures (Fig 17),

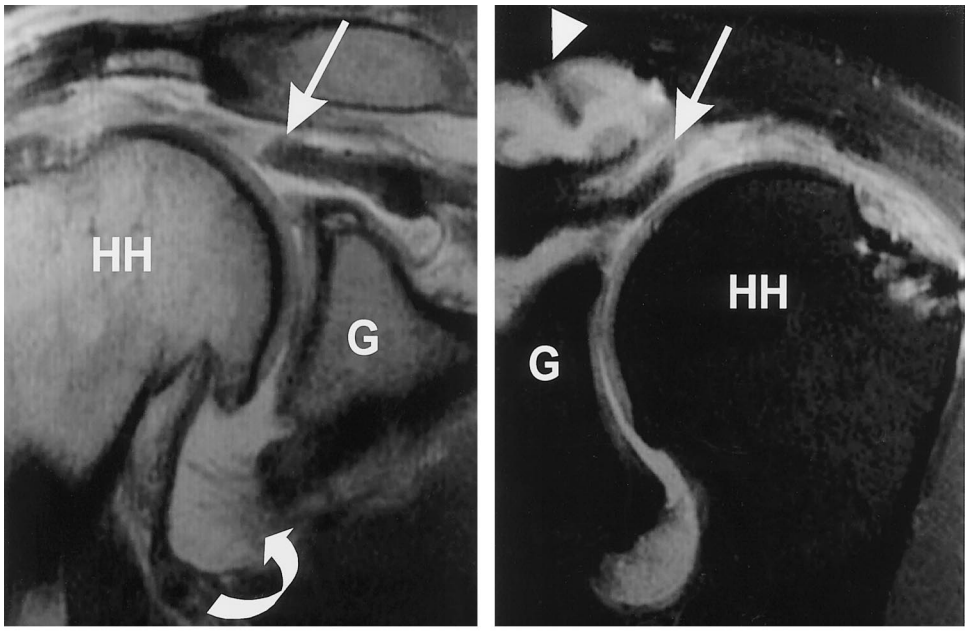

a. b.

Figure 18. Full-thickness recurrent tendon tear and retraction in a 49-year-old man with a history of rotator cuff repair. Coronal proton-density–weighted MR arthrograms obtained without **(a)** and with **(b)** fat suppression depict tendon retraction (straight arrow in **a**), associated synovitis (curved arrow in **a**), and the so-called geyser sign (arrow in **b**) produced by the extension of contrast material into acromioclavicular space (arrowhead in **b**) as a result of injury to the undersurface of the acromioclavicular joint. *G* = glenoid, *HH* = humeral head.

hardware displacement, heterotopic ossification, synovitis (Fig 18), and frozen shoulder (15–18). Defects in previously repaired rotator cuff tendons and capsulolabral structures are common complications and may be related to inadequate initial repair (Fig 19); poor-quality tendon, capsule, or bone; or improper physical therapy. The criteria for radiologic diagnosis of full-thickness recurrent tear of the rotator cuff are the presence of a cuff defect and the presence of fluid or contrast material in the tendinous gap (1) (Fig 18). Partial recurrent tears of the rotator cuff are difficult to distinguish from granulation tissue, fluid trapped in sutures, and full-thickness recurrent tears of the rotator cuff. In these instances the evaluation is remarkably improved with MR arthrography.

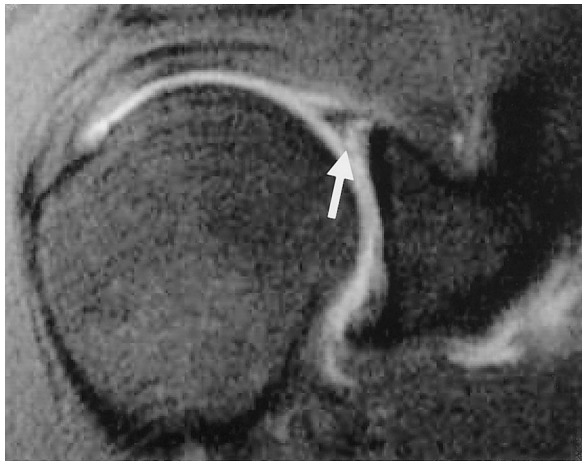

Figure 19. Superior labral tear in a middle-aged woman with persistent shoulder pain after arthroscopic subacromial decompression and rotator cuff repair. Coronal T1-weighted fat-suppressed MR arthrogram clearly shows the tear (arrow), which was missed during surgery.

Comparison of MR Imaging Techniques and Sequences

The diagnostic interpretation of images of the postoperative shoulder presents many challenges. Artifacts caused by ferromagnetic screws, staples, tacks, and small metal shavings from the use of surgical instruments, as well as anatomic distortion resulting from the surgical procedure, may make image interpretation difficult.

Local image distortions of two kinds may be caused by magnetic susceptibility effects depending on the imaging sequence used. The first kind of distortion, misregistration, affects spatial geometry and may appear on both spin-echo and gradient-echo images; the second kind of distortion, loss of signal intensity, is related to intravoxel dephasing (the so-called $T2^*$ effect) caused

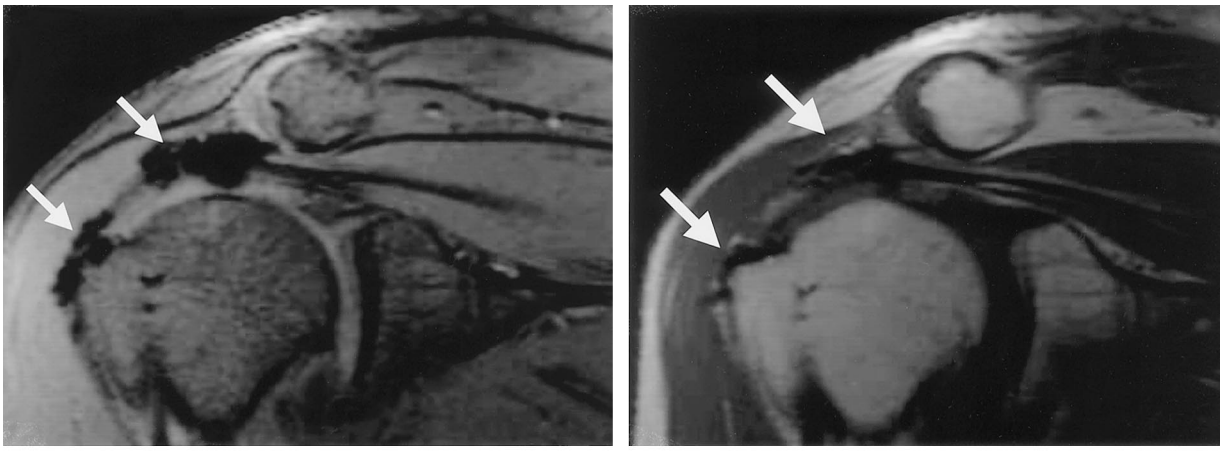

a. **b.**

Figure 20. Comparison of the severity of metallic artifacts on coronal MR images obtained with different pulse sequences. Magnetic susceptibility artifacts (arrows) obscure the underlying tendon on the gradient-echo image **(a)** but are barely noticeable on the proton-density–weighted image **(b).**

by the absence of the 180° refocusing pulse and appears only on gradient-echo images (19,20). With regard to the first type of distortion, misregistration is more severe on images obtained with a long echo time, because there is more time for protons to dephase. The protons acquire widely disparate precession frequencies and hence produce large cumulative phase errors. Low-signal-intensity magnetic susceptibility artifacts are more prominent on gradient-echo images than on images obtained with any other sequence (Fig 20). Gradient-echo images also may be distorted by blooming artifacts, which make bones appear larger and adjacent areas of soft tissue appear smaller than they are (21). In addition, fat saturation techniques may fail because of field inhomogeneity as a result of magnetic susceptibility. Several techniques can be used to minimize these artifacts: Inversion recovery may be used instead of fat saturation, fast spin-echo sequences may be used instead of standard spin-echo sequences, and gradient-echo sequences may be avoided (6,9,10).

MR arthrography has been used successfully for the evaluation of rotator cuff repairs and instability surgeries (11,13,21,22). At our institution, MR arthrography of the shoulder is routinely performed under fluoroscopic guidance and with either an anterior or a posterior needle entry site, depending on clinical symptoms and the surgical procedure performed (23). The MR arthrographic protocol includes T1-weighted fat-suppressed sequences applied in coronal, axial, and sagittal planes, with the arm in neutral position, as well as with the arm in a position of abduction and external rotation. In addition, a T2-weighted fat-suppressed sequence is applied in the coronal plane with the arm in neutral position. The T2-weighted fat-suppressed sequence with the arm in neutral position and the T1-weighted fat-suppressed sequence with the arm in abduction and external rotation are recommended for better delineation of the inferior glenohumeral ligament, anteroinferior labrum, and undersurface of the rotator cuff and for identification of native fluid in the subacromial-subdeltoid bursa and of ganglion cysts, respectively.

The advantages of MR arthrography over other MR imaging techniques include better definition of the rotator cuff, labral ligamentous structures, and tendon defects (Fig 21) and more accurate assessment of capsule volume (24–26). Although MR arthrography is not used in the evaluation of subacromial space and bursal-sided abnormalities of the rotator cuff, it can provide remarkably improved evaluation of the undersurface of the rotator cuff and aid in the differentiation of partial and full-thickness tears: Partial tears are characterized by contrast material filling a partial tendon defect; full-thickness tears are characterized by complete cuff defect with extravasation of contrast material to the subacromial-subdeltoid space (1,5,6). In addition, pitfalls of MR imaging can be avoided with MR arthrography. At MR imaging, scar tissue in the subacromial-subdeltoid space may fill a cuff defect and simulate tendon tissue. Secondary findings of full-thickness tear, such as medial retraction of the myotendinous junction or fluid in the subacromial-subdeltoid space and acromioclavicular joint, also may be unreliable if based on nonenhanced MR images.

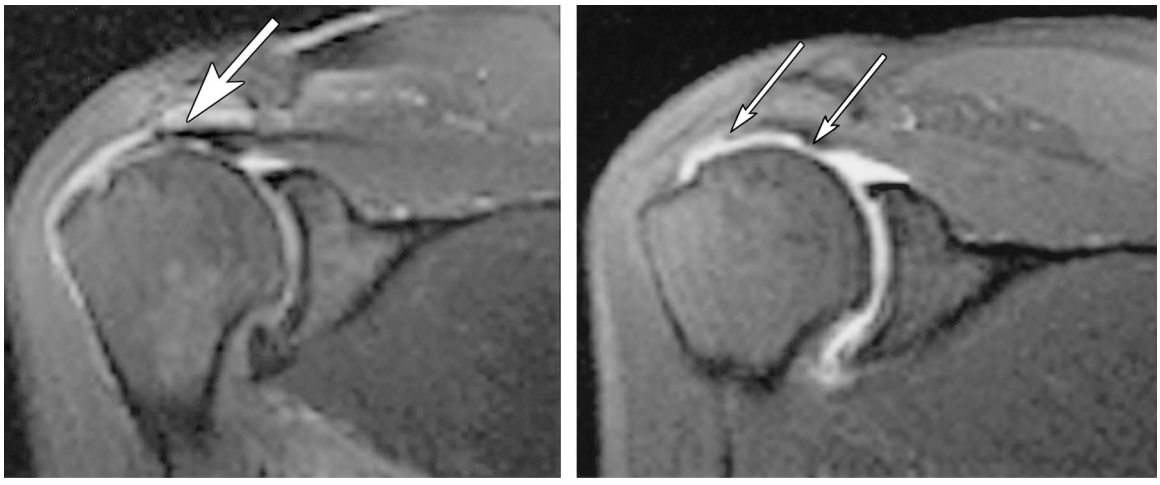

a. b.

Figure 21. Bursitis in a 63-year-old man after rotator cuff repair. **(a)** Coronal T2-weighted fat-suppressed image depicts heterogeneous signal intensity in the supraspinatus tendon (arrow) because of a moderate fluid accumulation in the subacromial-subdeltoid bursa, a finding indicative of a possible full-thickness tear at the attachment site. **(b)** Coronal T1-weighted fat-suppressed MR arthrogram depicts an irregular but intact tendon (arrows). Note the absence of contrast material in the subacromial-subdeltoid space.

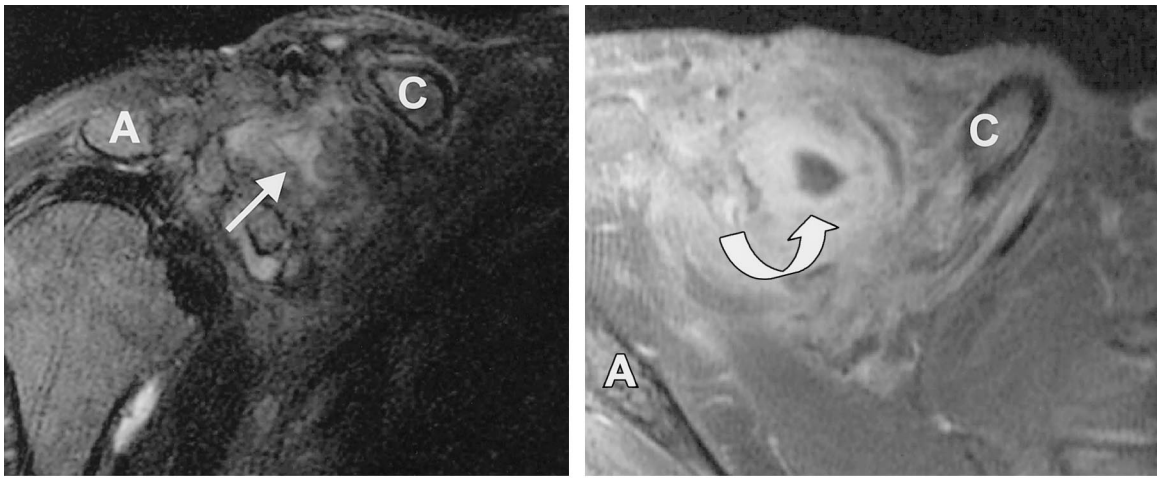

a. b.

Figure 22. Abscess in a middle-aged man after surgical reconstruction of the coracoclavicular ligament. **(a)** Coronal T2-weighted fat-suppressed image shows an area of high signal intensity (arrow) in the region of the coracoclavicular ligament. **(b)** Axial T1-weighted fat-suppressed image obtained after intravenous administration of gadolinium depicts an abscess in the region of the ligament (arrow) and enhancement of the surrounding tissues. *A* = acromion, *C* = clavicle.

The guidelines given earlier for the acquisition and interpretation of MR images of the postoperative shoulder should be applied also in the acquisition and interpretation of MR arthrograms. While correlating postoperative images with preoperative images, the radiologist should keep in mind the nature of the surgical procedures that have been performed: After nonanatomic procedures, capsular or labral abnormalities may persist. After anatomic procedures, there should be no separation between the capsulolabral complex and the glenoid margin. To better identify persistent abnormalities, MR arthrography should be performed during abduction and external rotation of the arm.

Standard MR imaging (T1-weighted fat-suppressed sequence) after intravenous gadolinium administration is usually used to confirm the presence of septic arthritis or abscess (Figs 16, 22).

Conclusions

In evaluation of the postoperative shoulder, choices among MR imaging sequences and techniques should be made carefully. To avoid magnetic susceptibility artifacts at MR imaging, inversion recovery may be used instead of fat saturation, and fast spin-echo sequences may be used instead of conventional spin-echo sequences or gradient-echo sequences. MR arthrography is most useful for optimal delineation of the rotator cuff, capsulolabral structures, and tendon defects. During image interpretation, postoperative and preoperative images should be correlated closely. Findings that are considered diagnostic or indicative of pathologic conditions in the preoperative shoulder may represent normal or improved conditions in the postoperative shoulder.

References

1. Resnick D. Shoulder. In: Resnick D, Kang HS, eds. Internal derangements of joints: emphasis on MR imaging. Philadelphia, Pa: Saunders, 1997; 163–333.
2. Arroyo JS, Flatow EL. Management of rotator cuff disease: intact and repairable cuff. In: Iannotti JP, Williams GR Jr, eds. Disorders of the shoulder: diagnosis and management. Philadelphia, Pa: Lippincott, Williams & Wilkins, 1999; 31–56.
3. Matsen FA, Arntz CT, Lippitt SB. Rotator cuff. In: Rockwood CE, Matsen FA, eds. The shoulder. Philadelphia, Pa: Saunders, 1998; 755–795.
4. Yamaguchi K. Mini-open rotator cuff repair: an updated perspective. Instr Course Lect 2001; 50: 53–61.
5. Stoller DW, Wolf EM. The shoulder. In: Stoller DW, ed. Magnetic resonance imaging in orthopaedics and sports medicine. 2nd ed. Philadelphia, Pa: Lippincott-Raven, 1997; 597–742.
6. Zlatkin MB. MRI of the postoperative shoulder. Skeletal Radiol 2002; 31:63–80.
7. Allain J, Goutallier D, Glorion C. Long-term results of the Latarjet procedure for the treatment of anterior instability of the shoulder. J Bone Joint Surg Am 1998; 80:841–852.
8. Lyons TR, Griffith PL, Savoie FH, Field LD. Laser-assisted capsulorrhaphy for multidirectional instability of the shoulder. Arthroscopy 2001; 17: 25–30.
9. Rand T, Trattnig S, Breitenseher M, Wurnig C, Marschner B, Imhof H. The postoperative shoulder. Top Magn Reson Imaging 1999; 10:203–213.
10. Haygood TM, Oxner KG, Kneeland JB, Dalinka MK. Magnetic resonance imaging of the postoperative shoulder. Magn Reson Imaging Clin N Am 1993; 1:143–155.
11. Spielmann AL, Foster BB, Kokan P, Hawkins RH, Janzen DL. Shoulder after rotator cuff repair: MR imaging findings in asymptomatic individuals—initial experience. Radiology 1999; 213:705–708.
12. Hashiuchi T, Ozaki J, Sakurai G, Imada K. The changes occurring after the Putti-Platt procedure using magnetic resonance imaging. Arch Orthop Trauma Surg 2000; 120:286–289.
13. Vahlensieck M, Lang P, Wagner U, et al. Shoulder MRI after surgical treatment of instability. Eur J Radiol 1999; 30:2–4.
14. Karas EH, Iannotti JP. Failed repair of the rotator cuff: evaluation and treatment of complications. J Bone Joint Surg Am 1997; 79:784–793.
15. Dawson J, Hill G, Fitzpatrick R, Carr A. Comparison of clinical and patient-based measures to assess medium-term outcomes following shoulder surgery for disorders of the rotator cuff. Arthritis Rheum 2002; 47:513–519.
16. Galatz LM, Griggs S, Cameron B, Iannotti JP. Prospective longitudinal analysis of postoperative shoulder function: a ten-year follow-up study of full-thickness rotator cuff tears. J Bone Joint Surg Am 2001; 83:1052–1056.
17. Kaar TK, Schenck RC, Wirth MA, Rockwood CA. Complications of metallic suture anchors in shoulder surgery: a report of 8 cases. Arthroscopy 2001; 17:31–37.
18. Wagner SC, Schweitzer ME, Morrison WB, Fenlin JM, Bartolozzi AR. Shoulder instability: accuracy of MR imaging performed after surgery in depicting recurrent injury—initial findings. Radiology 2002; 222:196–203.
19. Guermazi A, Miaux Y, Zaim S, Peterfy CG, White D, Genant HK. Metallic artefacts in MR imaging: effects of main field orientation and strength. Clin Radiol 2003; 58:322–328.
20. Peh WCG, Chan JHM. Artifacts in musculoskeletal magnetic resonance imaging: identification and correction. Skeletal Radiol 2001; 30:179–191.
21. Rand T, Freilinger W, Breitenseher M, et al. Magnetic resonance arthrography (MRA) in the postoperative shoulder. Magn Reson Imaging 1999; 17:843–850.
22. Sugimoto H, Suzuki K, Mihara K, Kubota H, Tsutsui H. MR arthrography of shoulders after suture-anchor Bankart repair. Radiology 2002; 224:105–111.
23. Chung CB, Dwek JR, Feng S, Resnick D. MR arthrography of the glenohumeral joint: a tailored approach. AJR Am J Roentgenol 2001; 177:217–219.
24. Beltran J, Bencardino J, Mellado JM, et al. MR arthrography of the shoulder: normal variants and pitfalls. RadioGraphics 1997; 17:1403–1412.
25. Stoller DW. MR arthrography of the glenohumeral joint. Radiol Clin North Am 1997; 35:97–115.
26. Binkert CA, Zanetti M, Gerber C, Hodler J. MR arthrography of the glenohumeral joint: two concentrations of gadoteridol versus Ringer solution as the intraarticular contrast material. Radiology 2001; 220:219–224.

This article meets the criteria for 1.0 credit hour in category 1 of the AMA Physician's Recognition Award. To obtain credit, see www.rsna.org/education/_cme.html.